Signature splitting of the $\pi h_{11/2}$ band and high-spin structures in ^{155}Tb*

LI Tao(李涛)[1;1)] CHEN Bao-Ren(陈宝仁)[1;2)] LIU Shu-Xin(刘树新)[1,2;3)]

[1] School of Physics, Peking University, Beijing 100871, China

[2] Center of Theoretical Nuclear Physics, National Laboratory of Heavy Ion Collisions, Lanzhou 730000, China

Abstract Seven experimentally observed bands of ^{155}Tb are analyzed in detail, using the particle-number-conserving method for treating the cranked shell model with monopole and quadrupole pairing interactions. We satisfactorily reproduce the experimental alignments and especially focus on the microscopic mechanism of the second back-bending and the influence of pair interaction on ultrahigh spins. Our calculated results show that the $\pi i_{13/2}$ orbitals are too high to give a contribution to the moment of inertia below $\hbar\omega \approx 0.7$ MeV. Instead, the crossing between the π[541]1/2 and other proton orbitals is responsible for the second back-bending. We assign a possible configuration to the decoupled band found in ^{155}Tb and predict eleven bands which are experimentally unobserved.

Key words rare-earth, high-j intruder orbital, alignment, particle-number-conserving method, back-bending

PACS 21.10.Re, 21.60.Cs, 27.70.+q

1 Introduction

The development of techniques in high-spin spectroscopy utilizing heavy-ion induced reactions has established the existence of some bands up to very high-spin states, which have provided a wealth of information on new nuclear structure phenomena. In the rare-earth region of the nuclear landscape nuclei can accommodate the highest values of angular momenta [1] and there are some central topics about these spectroscopy, such as superdeformed nuclei around ^{152}Dy, triaxial strongly deformed bands, second proton alignment, band termination in $N \sim 90$ nuclei. The $N = 90$ isotone chain is one of the most well studied groups of nuclei in the rare-earth region. These nuclei dwell within a highly transitional area of deformation space and are especially susceptible to shape driving forces by various competing processes. Previous high-spin studies of ^{155}Tb established rotational bands based on the [411]3/2, [532]5/2 and [413]5/2 proton states up to $I^\pi = \frac{75}{2}^+, \frac{95}{2}^-$ and $\frac{33}{2}^+$, respectively [2–5]. In the same region ($40\hbar < I < 50\hbar$), there are band terminating states in nearby nuclei [6, 7] and new band structures in ^{157,158}Er established to ultrahigh spin ($> 60\hbar$) bypass and extend beyond these band terminating states [1]. In this paper we will analyze high-spin structures in ^{155}Tb and investigate the rotational alignment of specific pairs of quasiparticles, using the particle-number-conserving (PNC) method for treating the cranked shell model (CSM) with monopole and quadrupole pairing interactions. The second back-bending was discovered in 1977 [8] and since then its study has provided detailed information concerning the single-particle levels in the second back-bending frequency region.

In our PNC calculations, we will focus on the high-spin behavior of all rotational alignments based on different configurations. The PNC method is given in Sec. 2. The parameters that we use in our calculation are given in Sec. 3. Two pairs of signature partner bands based on the [411]3/2 and [413]5/2 proton states are discussed in 3.1. The [532]5/2 band, where the second back-bending band appears, is analyzed

Received 10 August 2009

* Supported by National Natural Science Foundation of China (10675006)

1) E-mail: litao120828@163.com

2) E-mail: baorench@gmail.com

3) E-mail: liusx@pku.edu.cn

in Part 3.2. In Part 3.3, a 3 quasiparticle band is assigned as a possible configuration and the theoretically predicted results are discussed.

2 The PNC method

The cranked shell model Hamiltonian with pairing interactions is given by

$$H_{\rm CSM} = H_{\rm SP} - \omega J_x + H_{\rm P} = H_0 + H_{\rm P}, \qquad (1)$$

where $H_0 = H_{\rm SP} - \omega J_x = \sum_i h_0(\omega)_i$, $h_0(\omega) = h_{\rm Nilsson} - \omega j_x$ is the one-body part of $H_{\rm CSM}$, $h_{\rm Nilsson}$ is the Nilsson Hamiltonian, $-\omega J_x$ the Coriolis interaction and $H_{\rm P}$ the pairing interaction including both the monopole and quadrupole pairing interactions [9, 10]. The Nilsson (modified oscillator) potential has been quite successful in describing the properties of superdeformed bands [11–13]. In the PNC treatment, first, $h_0(\omega)$ is diagonalized to obtain the cranked Nilsson orbits. Then, $H_{\rm CSM}$ is diagonalized in a sufficiently large cranked many-particle configuration (CMPC) space [14] to obtain the yrast and low-lying eigenstates. For the details of the PNC method, see Refs. [15–17]. Assuming that an eigenstate of $H_{\rm CSM}$ is expressed in terms of the CMPCs:

$$|\psi\rangle = \sum_i C_i |i\rangle , \qquad (2)$$

where $|i\rangle$ denotes an occupation of particles in cranked orbits and C_i is the corresponding probability amplitude. The occupation probability of the cranked orbital μ (including both signatures $\alpha = \pm 1/2$) is

$$n_\mu = \sum_i |C_i|^2 P_{i\mu} , \qquad (3a)$$

$$P_{i\mu} = \begin{cases} 1, \text{ if } |\mu\rangle \text{ is occupied in the CMPC } |i\rangle \\ 0, \text{ otherwise} \end{cases} . \qquad (3b)$$

The angular momentum alignment for the state $|\psi\rangle$ is $\langle J_x\rangle = \langle\psi| J_x |\psi\rangle$, and its kinematic MOI (moment of inertia) is $J^{(1)} = \langle J_x\rangle/\omega$. Because J_x is a one-body operator, the angular momentum alignment of the state $|\psi\rangle$ is

$$\langle J_x\rangle = \sum_\mu j_x(\mu) + \sum_{\mu<\nu} j_x(\mu\nu) , \qquad (4)$$

$$\begin{aligned} j_x(\mu) &= \langle\mu| j_x |\mu\rangle n_\mu, \\ j_x(\mu\nu) &= 2\langle\mu| j_x |\nu\rangle \sum_{i<j} (-)^{M_{i\mu}+M_{j\nu}} C_i^* C_j, \qquad (5) \\ & (\mu \neq \nu), \end{aligned}$$

where $j_x(\mu)$ is the direct contribution to $\langle J_x\rangle$ from a particle occupying the cranked orbital μ and $j_x(\mu\nu)$ is the contribution to $\langle J_x\rangle$ from the interference between two particles occupying the cranked orbitals μ and ν, which has no counterpart in the mean-field (BCS) treatment. Calculations show that $j_x(\mu\nu)$ plays an important role for the odd-even difference and non-additivity in the moments of inertia [18].

3 Rotational bands in ^{155}Tb

In the calculation of the bands [411]3/2 and [413]5/2, we use the deformation parameters $\varepsilon_2 = 0.225$, $\varepsilon_4 = -0.04$, which are a little higher than the other bands for which the parameters ($\varepsilon_2 = 0.216$, $\varepsilon_4 = -0.033$) are taken from the Lund systematics [19]. This change of deformation parameters is due to the only up-bending observed in the band [411]3/2 and [413]5/2, while a slight backbend was observed in the [532]5/2 band [19]. The Nilsson parameters (κ, μ) are taken from the Lund systematics too. They are slightly adjusted to make sure that the cranked proton Nilsson orbitals are consistent with the experimental data near the Fermi surface of ^{155}Tb. The corresponding effective pairing interaction strengths, G_0 (monopole) and G_2 (quadrupole) (in units of MeV) are determined by the experimental odd–even differences in the nuclear binding energies and bandhead moments of inertia: $G_{0\rm p} = 0.4$, $G_{2\rm p} = 0.015$ for protons; $G_{0\rm n} = 0.628$, $G_{2\rm n} = 0.018$ for neutrons respectively. For a larger truncated CMPC space, the effective pairing interaction strength will correspondingly decrease, but the calculated results for the yrast and low-lying eigenstates keep almost unchanged [20].

In order to simplify the following discussion, the quasiparticle orbitals have been labeled in the usual alphabetic manner [19, 21, 22]. The quasineutron orbitals are labeled with respect to parity and signature $(\pi, \alpha)_{\rm n}$ as

$$A = (+,+1/2)_1,\ C = (+,+1/2)_2,\ E = (-,+1/2)_1,$$

$$B = (+,-1/2)_1,\ D = (+,-1/2)_2,\ F = (-,-1/2)_1.$$

The subscript n numbers the quasiparticles' excitations of a specific signature and parity, starting with the lowest energy. The quasiproton orbitals are labeled as

$$A_{\rm p} = (-,-1/2)_1,\quad C_{\rm p} = (-,-1/2)_2,$$

$$E_{\rm p} = (+,+1/2)_1,\quad G_{\rm p} = (+,+1/2)_2$$

$$B_{\rm p} = (-,+1/2)_1,\quad D_{\rm p} = (-,+1/2)_2,$$

$$F_{\rm p} = (+,-1/2)_1,\quad H_{\rm p} = (+,-1/2)_2$$

Using this quasiparticle labeling scheme of the standard CSM, the seven rotational bands in ^{155}Tb are the following: the yrast positive-parity [411]3/2[$E_p(F_p)$], [413]5/2[$G_p(H_p)$], negative-parity [532]5/2 [$A_p(B_p)$] and 3-quasiparticles band $A_p \otimes AF$ respectively.

The cranked neutron and proton Nilsson orbits near the Fermi surface of the ^{155}Tb are shown in Fig. 1. From Fig. 1 we see that ν[660]1/2 is below

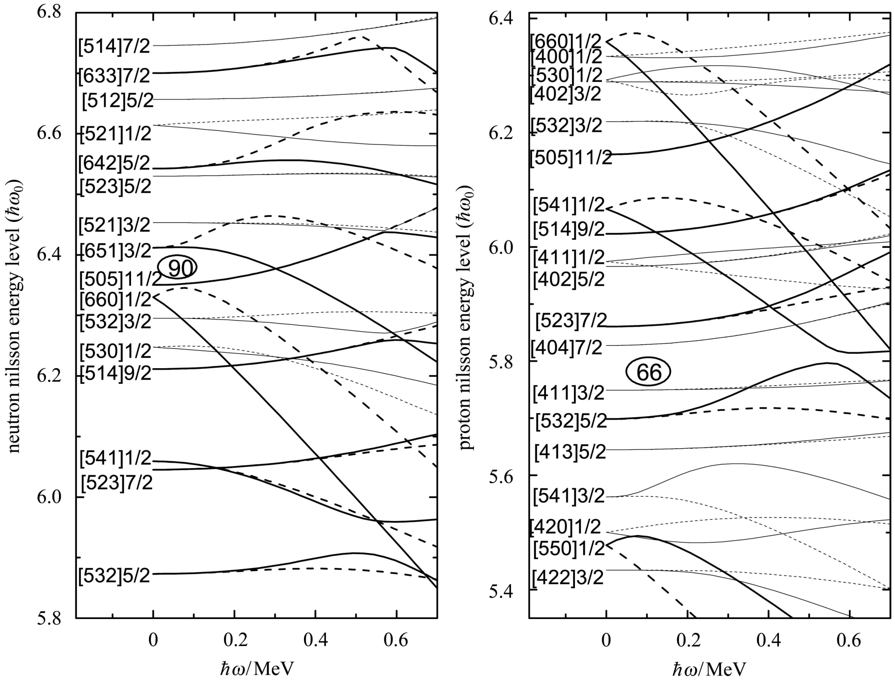

Fig. 1. The cranked proton and neutron Nilsson orbitals near the Fermi surface of ^{155}Tb. The signature $\alpha = \pm 1/2$ orbitals are denoted by solid and dashed lines, respectively. The high j orbitals are denoted by bold lines. In the calculation we used the deformation parameters $\varepsilon_2 = 0.216$, $\varepsilon_4 = -0.033$ from the Lund systematics.

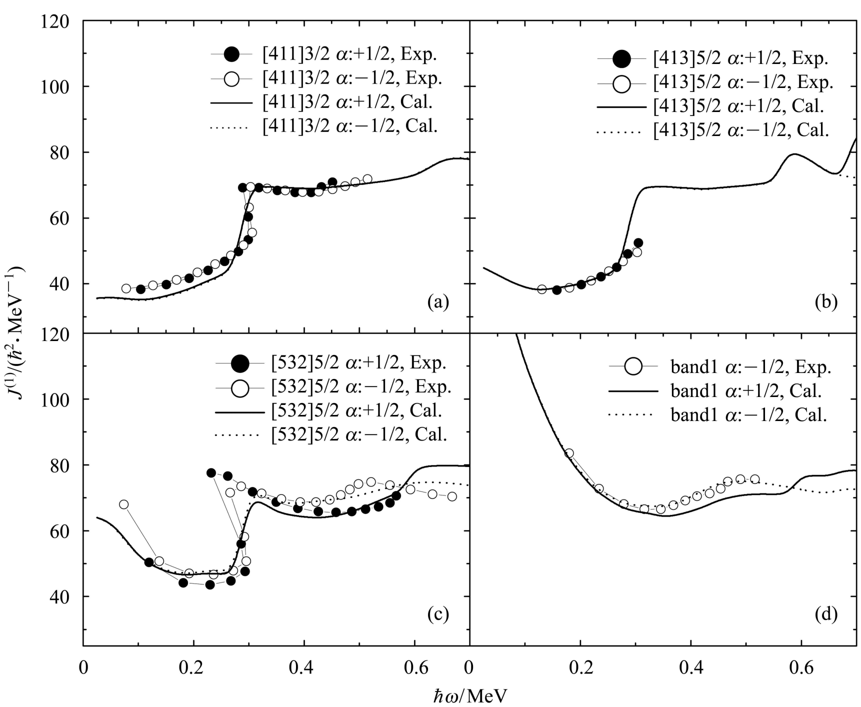

Fig. 2. Comparison between the experimental and calculated kinematic MOI $J^{(1)}$ of the seven rotational bands in ^{155}Tb. The experimental data are denoted by solid and open circles respectively. The calculated results for these bands are denoted by solid and dashed lines respectively.

the neutron Fermi surface, thus the interaction between ν[660]1/2 and other orbitals occurs easily. Although π[541]1/2 is far from the proton Fermi surface at low spins, it can cross with other orbitals at high cranking frequencies. The π[660]1/2 orbital is so far from the Fermi surface that it doesn't have any contribution in this region. In fact, our calculation shows that, if π[660]1/2 has any contribution in this frequency region, the alignment of the [532]5/2 $\alpha = +1/2$ band would be larger than that of the $\alpha = -1/2$ one, but this will contradict the experimental result.

The comparison between the calculated and experimental MOI of seven bands is shown in Fig. 2. The overall agreement between the calculated and experimental results is satisfactory. In this paper we mainly focus on the microscopic mechanism of the second back-bending of the [532]5/2 band, indicating that the π[660]1/2 orbital doesn't have any influence in the frequency range $\hbar\omega \approx$ 0.4–0.6 MeV, instead, π[541]1/2 will take the role of π[660]1/2.

3.1 The [411]3/2 and [413]5/2 band

In the calculation of the bands [411]3/2 and [413]5/2, the contributions of neutrons and protons to the MOI of these four bands are shown in Fig. 3. We see that the sharp increase of the MOIs of these four bands at $\hbar\omega \approx 0.3$ MeV mainly comes from the contributions of the neutron $N = 6$ shell (see Fig. 3(a)). At higher frequencies ($\hbar\omega > 0.5$ MeV), the alignment changes come from the proton $N = 5$ shell, the contributions of the proton $N = 4$ shell are small and constant (see Fig. 3(b), (c), (d) and (e)).

A high-j intruder orbital is characterized by its large Coriolis response and large contributions to the alignment at low frequencies. Thus the change of alignment at the region of backbending is mainly due to the excitations of high-j orbitals. According to the PNC calculations, the total increase of the first back-bending at $\hbar\omega \approx 0.3$ MeV is about $8.0\hbar$, while the increase of alignment coming from ν[660]1/2 is about $2.4\hbar$, the interaction between ν[651]1/2 and ν[660]1/2, ν[642]5/2 and ν[651]3/2 contributes $4.2\hbar$. The neutron N=5 shell contributes about $-0.3\hbar$. The contribution from protons is only $0.98\hbar$. Therefore, the contributions to the first back-bending come mainly from the alignment of the $\nu i_{13/2}$ orbitals. We can also conclude that the slight increase of alignment at $\hbar\omega \approx 0.6$ MeV comes from the proton $N = 5$ shell, similar to the [413]5/2 band at $\omega \approx 0.525$ MeV, both are mainly due to the crossing between π[541]1/2 and π[532]5/2.

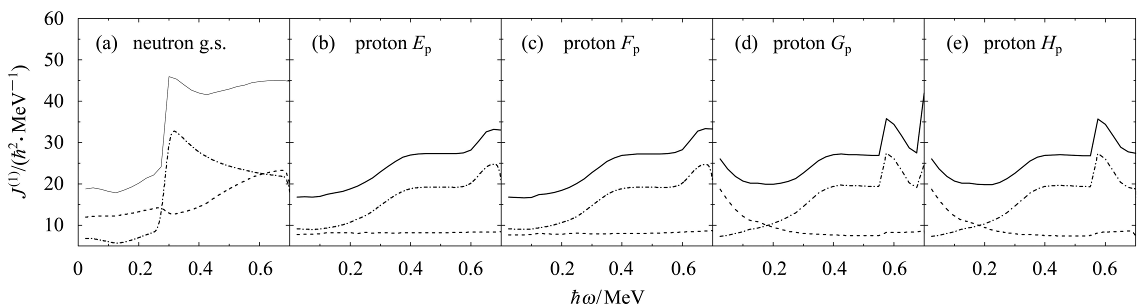

Fig. 3. The contributions to the kinematic MOI $J^{(1)}$ from: (a) neutron configuration $(+,0)_1$; (b) proton configuration E_p; (c) proton configuration F_p; (d) proton configuration G_p (e) proton configuration H_p respectively in ^{155}Tb. The dash dotted lines represent $N = 6$ for neutrons, $N = 5$ for protons, and the dashed lines represent $N = 5$ for neutrons, $N = 4$ for protons.

3.2 The [532]5/2 band

Figure 2(c) shows the comparison between the experimental and calculated MOI of the [532]5/2 band. Both signatures experience a slight backbending in the AB crossing at $\hbar\omega \approx 0.28$ MeV and an alignment gain of $9.3\hbar$ was observed in each signature. The contributions of neutrons and protons to the MOI of these two bands, based on π[532]5/2, are shown in Fig. 4. The sharp increase of the MOI of the [532]5/2 band at $\hbar\omega \approx 0.28$ MeV mainly comes from the contributions of the neutron $N = 6$ shell similar to the bands [411]3/2 and [413]5/2 (see Fig. 4(a)). From Fig. 2(c) we also see that at $\hbar\omega < 0.4$ MeV the signature splitting and inverse between A_pB_p can't be reproduced by our PNC calculation, however at $\hbar\omega >$ 0.4 MeV the overall agreement is good. The orbital occupation probabilities of the proton $N = 5$ shell show that the signature splitting at $\hbar\omega > 0.4$ MeV is mainly caused by the crossing between the proton orbital [541]1/2 and other orbitals which are near the Fermi surface.

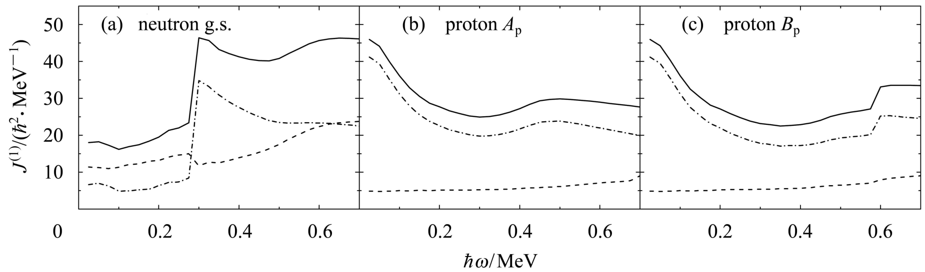

Fig. 4. The contributions to the kinematic MOI $J^{(1)}$ from: (a) quasineutron vacuum configuration $(+,0)_1$; (b) proton configuration A_p; (c) proton configuration B_p in ^{155}Tb. The dash dotted lines represent $N=6$ for neutrons, $N=5$ for protons, and the dashed lines represent $N=5$ for neutrons, $N=4$ for protons.

Another crossing of the $\alpha=-1/2$ signature occurs at $\hbar\omega \approx 0.47$ MeV and is regarded as the alignment of the B_p and C_p protons. Our calculated results show that the alignment of the proton $N=5$ shell decreases with the rotational frequencies at low spins and increases beyond $\hbar\omega\approx 0.40$ MeV earlier than the experimental result (see Fig. 4(b)).

The $\alpha=+1/2$ signature of the [532]5/2 band begins to gain alignment at very high rotational energy, $\hbar\omega \approx 0.57$ MeV. The $\alpha=-1/2$ signature does not experience any kind of crossing in this frequency region, which implies that this is most likely the A_pD_p crossing [2]. Our calculated results show that π[541]1/2 is responsible for this crossing. Although π[541]1/2 is far from the proton Fermi surface at low spins, it declines with cranked frequencies and interacts with π[523]7/2 and π[532]5/2, one after the other, (see Fig. 1). The B_p's alignment has a gain coming from the contribution of the proton $N=5$ shell at $\hbar\omega \approx 0.57$ MeV (see Fig. 4(c)). In the $\hbar\omega \approx 0.57$ MeV frequency region, the occupation probabilities of π[523]7/2 and π[532]5/2 increase while those of π[411]3/2 decreases rapidly. It is worthwhile to note that according to the Lund systematics, π[660]1/2 has a crossing at $\hbar\omega\approx 0.57$ MeV, instead of π[541]1/2, but this contradicts the experimental result. This case suggests that the Lund systematics needs to be modified.

3.3 Band 1 and predicted bands

With the lowest observed state at 2745.2 keV and spin $I=27/2$, Band 1 is tentatively regarded as a candidate for a three-quasiparticle band which likely involves an $h_{11/2}$ proton since it decays into the [532]5/2 band and has been assigned as the $A_p \otimes AF$ configuration [2]. The lowest excited state meeting this assignment is the ν[651]3/2ν[505]11/2⊗π[532]5/2 configuration (see Fig. 1). According to our PNC calculations, the occupation probability of ν[651]3/2 and ν[505]11/2 in the two-quasiparticle state $(-,0)_1$ is about 1 for all the cranked frequencies, the overall agreement between the experiment and calculations being very good (see Fig. 2(d)). The larger bandhead MOI of Band 1 comes from the neutron $N=6$ shell and it may also experience an A_pD_p crossing at $\hbar\omega\approx 0.57$ MeV.

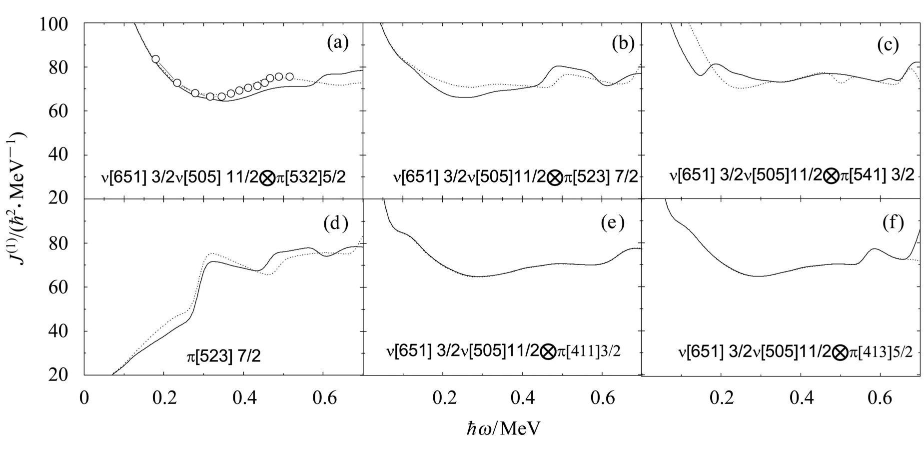

Fig. 5. The predicted variations of the kinematic MOI $J^{(1)}$ of other bands with ω in ^{155}Tb. $\alpha=\pm 1/2$ of each band is denoted by the solid and dashed lines respectively.

Besides the analysis of the experimentally observed rotational bands, we further predict the unobserved eleven bands shown in Fig. 5. The only band not including the high-j intruder orbital is the π[523]7/2 band, see Fig. 5(d). Our calculated result shows that the [541]3/2 proton and the interference between [523]7/2 and [532]5/2 are responsible for the smaller bandhead MOI of these two bands. For the first backbending of the this band, according to the PNC calculations, the contributions to the first backbending comes mainly from the alignment of the $\nu i_{13/2}$ orbitals.

4 Summary

We analyze the seven experimentally observed bands of ^{155}Tb in detail using the PNC method. We satisfactorily reproduce the experimental alignments and especially focus on the microscopic mechanism of the second back-bending of the [532]5/2 band, which first confirms the order of Nilsson single-particle level at higher cranked frequencies. Our calculated results show that the $\pi i_{13/2}$ orbits are too high to contribute to the MOI below $\hbar\omega \approx 0.7$ MeV. Instead, the crossing between π[541]1/2 and other proton orbits is responsible for the second back-bending. According to the Lund systematics, π[660]1/2 shows this crossing at $\hbar\omega \approx 0.57$ MeV, instead of π[541]1/2. This contradiction suggests that the Lund systematics needs to be modified. We also assign a possible configuration to the decoupled band found in ^{155}Tb. In addition, we predict eleven bands which are experimentally unobserved and assign their possible configurations.

References

1 Paul E S, Twin P J, Evens A O. Phys. Rev. Lett., 2007, **98**: 012501-1–4

2 Hartley D J, Brown T B, Kondev F G et al. Phys. Rev. C, 1998, **58**: 2720–2735

3 Winter G, Funke L, Kaun K H et al. Nucl. Phys. A, 1971, **176**: 609–625

4 Tippett J C, Burke D G. Can. J. Phys., 1972, **50**: 3152–3171

5 Riley M A, Hartley D J, Simpson J et al. Phys. Rev. C, 1996, **53**: 989–992

6 Evens A O, Paul E S, Simpson J et al. Phys. Rev. Lett., 2004, **92**: 252502-1–4

7 Evens A O, Paul E S, Simpson J et al. Phys. Rev. C, 2006, **73**: 064303-1–14

8 Lee J Y, Aleonard M M, Deleplanque M A et al. Phys. Rev. Lett., 1977, **38**: 1454–1457

9 Wakai M, Faessler A. Nucl. Phys. A, 1978, **295**: 86–110

10 Dibel M. Nucl. Phys. A, 1984, **419**: 221–240

11 Ragnarsson I. Nucl. Phys. A, 1993, **557**: 167–177

12 Karlsson L B, Ragnarsson I, Aerg S. Nucl. Phys. A, 1998, **639**: 654–682

13 Afanasjev A V, Ragnarsson I, Ring P. Phys. Rev. C, 1999, **59**: 3166–3171

14 WU C S, ZENG J Y. Phys. Rev. C, 1989, **39**: 666–670

15 ZENG J Y, JIN T H, ZHAO Z J. Phys. Rev. C, 1994, **50**: 1388–1397

16 ZENG J Y, LIU S X, LEI Y A, YU L. Phys. Rev. C, 2001, **63**: 024305-1–4

17 XIN X B, LIU S X, LEI Y A, ZENG J Y. Phys. Rev. C, 2000, **62**: 067303-1–4

18 LIU S X, ZENG J Y. Phys. Rev. C, 2002, **66**: 067301-1–4

19 Bengtsson R, Frauendorf S, May F R. At. Data Nucl. Data Tables, 1986, **35**: 15–122

20 LIU S X, ZENG J Y, ZHAO E G. Phys. Rev. C, 2002, **66**: 024320-1–5

21 Bengtsson R, Frauendorf S. Nucl. Phys. A, 1979, **314**: 27–36; Bengtsson R, Frauendorf S. Nucl. Phys. A, 1979, **327**: 139–171

22 Riedinger L L, Andersen O, Frauendorf S et al. Phys. Rev. Lett., 1980, **44**: 568–572